Kinetic Studies of the Deactivation of $O_2(^1\Sigma_g^+)$ and $O(^1D)$

JICHUN SHI and JOHN R. BARKER

Department of Atmospheric, Oceanic and Space Sciences, Space Physics Research Laboratory, The University of Michigan, Ann Arbor, Michigan 48109-2143

Abstract

The kinetics of the deactivation of $O_2(^1\Sigma_g^+)$ is studied in real time. $O_2(^1\Sigma_g^+)$ is generated in this system by the $O(^1D) + O_2$ reaction following O_3 laser flash photolysis in the presence of excess O_2, and it is monitored by its characteristic emission band at 762 nm. Quenching rate constants were obtained for O_2, O_3, N_2, CO_2, H_2O, CF_4 and the rare gases. Since $O(^1D)$ is the precursor for the formation of $O_2(^1\Sigma_g^+)$, the addition of an $O(^1D)$ quencher effectively lowers the initial concentration of $O_2(^1\Sigma_g^+)$. By measuring the initial intensity of the 762 nm fluorescence signal, the relative quenching efficiencies were determined for $O(^1D)$ quenching by N_2, CO_2, Xe, and Kr with respect to O_2; the results are in good agreement with literature values.

Introduction

The two low-lying excited electronic states of oxygen, $O_2(^1\Sigma_g^+)$ and $O_2(^1\Delta_g)$, are of considerable interest, because they play important roles in the chemistry of the upper atmosphere [1]. Due to the strong selection rules prohibiting their radiative and collisional transitions, they have very long lifetimes in the atmosphere. $O_2(^1\Sigma_g^+)$ has been observed in both the ambient upper atmosphere [2] and in the aurora [3]. The daytime and night-time production mechanisms for $O_2(^1\Sigma_g^+)$ have been studied in the laboratory and tested very extensively in field observations [1,4,5].

The $O_2(^1\Sigma_g^+)$ deactivation process has been studied many times in the past, and has been reviewed recently by Wayne [6]. Two approaches were usually used for these studies: the first approach [7–10] uses microwave discharge of O_2 to generate $O_2(^1\Sigma_g^+)$ and $O_2(^1\Delta_g)$ in a slow flow system. Under the experimental conditions in these studies, the $O_2(^1\Sigma_g^+)$ molecules observed are mainly from the energy pooling reaction of $O_2(^1\Delta_g)$. By monitoring the 762 nm emission band from $O_2(^3\Sigma_g^- \leftarrow {}^1\Sigma_g^+)$ at various reaction times with and without quenching molecules, the quenching rates can be obtained using the Stern-Volmer method. The basic requirements for this technique are that the wall deactivation rates and the mechanism for the generation of $O_2(^1\Sigma_g^+)$ in the reaction zone be known accurately.

In the second approach, which has been developed more recently, $O_2(^1\Sigma_g^+)$ is generated following the flash (or laser flash) photolysis of O_3 or O_2 in the presence of a large excess of O_2. Under these experimental conditions, $O(^1D)$ produced by photodissociation reacts with O_2 to produce $O_2(^1\Sigma_g^+)$:

$$O(^1D) + O_2 \longrightarrow O_2(^1\Sigma_g^+) + O \quad (1)$$

International Journal of Chemical Kinetics, Vol. 22, 1283–1301 (1990)
 CCC 0538-8066/90/121283-19$04.00

The efficiency of $O_2(^1\Sigma_g^+)$ production in this reaction has been determined in previous studies to be 0.77 ± 0.2 [11,12]. Since this formation reaction is very fast, the decay of $O_2(^1\Sigma_g^+)$ can be monitored directly in real time by the characteristic emission band at 762 nm, and this technique tends to eliminate the need to consider wall deactivation of $O_2(^1\Sigma_g^+)$.

$O_2(^1\Sigma_g^+)$ deactivation rate constants obtained from the two approaches described above are generally in good agreement, but small differences exist. For example, the $O_2(^1\Sigma_g^+)$ deactivation by CO_2 has been measured in several studies, but the two most recent ones seem to give smaller rate constants [13,14]; due to its importance in the atmospheres of Mars and Venus, it is worthwhile to investigate this reaction again. The deactivation of $O_2(^1\Sigma_g^+)$ by rare gases has been assumed to be inefficient in most kinetic studies in the past, but very few actual measurements have been made; real time measurements of these rate constants are reported here.

Theoretical studies of the electronic deactivation of $O_2(^1\Sigma_g^+)$ have been carried out by several groups [15,16]. Kear and Abrahamson [15] assumed that energy is transferred under the influence of the short range repulsive forces and, when rotational effects are neglected, this model correctly predicts the trends in the deactivation rate constants for most colliders, but the absolute values are one or two orders of magnitude too small. In a more recent study, Braithwaite, Davidson, and Ogryzlo [16] considered long range interactions due to the attractive part of the intermolecular potential energy curve, and their calculated rate constants agree reasonably well with experimental values, but as pointed out by Borrell, Borrell, and Grant [7], neither of the above approaches can explain the observed temperature dependence. Borrell, et al. used in a general curve-crossing approach, and found that the crossing probably occurs near the shallow minimum of the intermolecular potential energy curve. Thus, this process is particularly sensitive to the nature of the quencher.

The reactions of $O_2(^1\Sigma_g^+)$ determine not only its behavior in the atmosphere, but they also affect other excited species in the atmosphere and in laboratory systems. $O_2(^1\Sigma_g^+)$ has an excitation energy of ca. 13,120 cm^{-1}, and part of this excitation energy may be transferred to other species during collisions. For example, the E-V transfer from $O_2(^1\Sigma_g^+)$ to CO_2 has been found in several studies to produce $CO_2(101)$ or $CO_2(02^01)$ [17,18]. $O_2(^1\Sigma_g^+)$ E-V transfer processes involving H_2O, HCl and other colliders have also been investigated. These energy transfer processes may be important in the infrared airglow of the Earth and other planets.

For some colliders (e.g., O_2, N_2, and CO_2), the deactivation of $O_2(^1\Sigma_g^+)$ produces $O_2(^1\Delta_g)$, while for other colliders, chemical reactions may take place. One example of such reactions is that between $O_2(^1\Sigma_g^+)$ and O_3, which has been studied many times before. Excellent agreement exists among the kinetic measurements, but the products are still not well understood. Slanger and Black [19] studied this reaction by directly monitoring O atom growth by the resonance absorption method, and their results indicate that only 2/3 of this reaction produces O atom. This finding has been confirmed by Amimoto and Wiesenfeld [20]. Furthermore, recent studies of the infrared fluorescence from the O + O_2 + Ar reaction system in the 9–12 μm region carried out by Rawlins, Caledonia, and Armstrong [21] have indicated that

vibrationally excited ozone in levels as high as $O_3(005)$ may be produced from the reaction between $O_2(^1\Sigma_g^+)$ and O_3.

A current investigation in this laboratory of infrared emission from $O_3 + O_2$ mixtures following laser excitation has revealed that several IR emission bands are produced in this system. In particular, an emission band centered near 1.9 μm has been discovered and studied [22]. The Noxon band of $O_2(^1\Sigma_g^+)$ is centered very close to this wavelength region [23], but the kinetics results obtained in our laboratory differ significantly from those of $O_2(^1\Sigma_g^+)$, based on the results of previous studies. Both the 762 nm emission band and the Noxon band at 1.91 μm have been used to monitor $O_2(^1\Sigma_g^+)$ in previous kinetic studies, and results from both emission bands have been found to agree with each other reasonably well [6]. An important motivation for the present study is to determine whether the newly-discovered 1.9 μm emission band is due to $O_2(^1\Sigma_g^+)$. Direct observation of the characteristic emission band at 762 nm gives unambiguous determination of the deactivation rate constants of $O_2(^1\Sigma_g^+)$ in this system, and the results reported here confirm that the 1.9 μm emission band observed in our other experiments is not due to emission from $O_2(^1\Sigma_g^+)$.

Since $O_2(^1\Sigma_g^+)$ in this study is produced by the $O(^1D) + O_2$ reaction following O_3 laser flash photolysis in excess O_2, the addition of an $O(^1D)$ quencher reduces the initial $O_2(^1\Sigma_g^+)$ concentration. By measuring the initial intensity of the 762 nm fluorescence signal, the relative quenching efficiencies of $O(^1D)$ have been determined for several molecules, with respect to quenching by O_2. In the following sections, we first describe the experimental system briefly, and then the 762 nm band kinetic results are presented and compared with those in the literature.

Experimental

The experimental arrangement for this study is shown schematically in Figure 1. The fluorescence cell is a 48 cm long stainless steel tube, with an inner diameter of 3.8 cm. A high concentration of O_3 was stored in the cell and after about 24 h of passivation, the dissociation of ozone on the cell walls (dark loss) was negligible. The laser beam at 308 nm is generated by a Lumonics XeCl excimer laser (HyperEx-400), with a beam diameter of ca. 1.5 cm and intensity of ca. 10 mJ/pulse before entering the cell. The laser intensity exiting the cell was monitored continuously by a power meter (Scientech 38-0102).

The characteristic emission band of $O_2(^1\Sigma_g^+)$ at 762 nm is monitored by a photomultiplier (Hamamatsu, R456) operated by a DC bias voltage of -850 V, and loaded with a 536 Ω resistor. The photomultiplier output signal is amplified by a Tektronix preamplifier (AM502) before being captured by a digital oscilloscope-signal averager (LeCroy 9400) for data acquisition and signal averaging. Under typical experimental conditions, signal averaging of about 5,000 laser shots is required to achieve a good signal to noise ratio. The signal may then be plotted with an online plotter (HP 7470A) and stored with a laboratory computer (Macintosh SE) for data analysis. The combined detection system has a response time of ca. 0.6 μs, which is limited mostly by the Tektronix preamplifier.

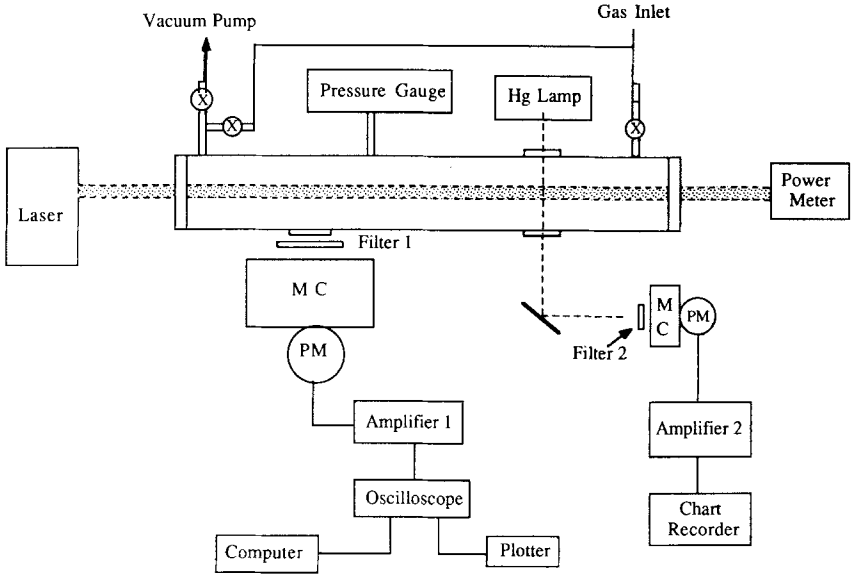

Figure 1. Schematic for the experimental apparatus; PM: photomultiplier; MC: monochromator.

In order to avoid scattered laser light, a 700 nm long-pass filter is used along with a monochromator. The slits on the monochromator are wide open in order to gain good optical throughput and the halfwidth of the transmitted light is ca. 18 nm, according to calibrations with a He-Ne laser. Because of intense laser radiation in the experiments, the scattered light cannot be eliminated completely despite exhaustive efforts, but the interference is confined to the first 2 μs. The scattered light signal from a blank run is subtracted from every measurement run; as will become clear later in this report, these efforts effectively eliminate interference from the scattered laser light.

The gases used here are of ultrapure grade and, whenever possible, are passed through a dry ice cooled silica gel trap in order to remove impurities such as H_2O. Ozone is produced with a silent ozonizer and stored on a silica gel trap at dry ice temperature. The pressure of collider gas is measured by a MKS pressure transducer (0–1000 torr) and the measurement is accurate to ± 0.1 torr according to the manufacturer's specifications; the transducer linearity up to 1200 torr was confirmed in laboratory calibrations. The partial pressure of ozone is monitored by the attenuation of 2537 Å light from a low pressure Hg lamp. The ozone absorption cross section at this wavelength is 1.14×10^{-17} cm^2 at room temperature [24,25]. For O_3 partial pressures less than 1 torr, the absorption obeys Beer's Law.

Gas mixtures are prepared in two different ways: in one method, the $O_3 + O_2$ mixture from the ozonizer flows slowly through the cell with flow rate between 5 and 45 scc/s, depending on total pressure (the cell volume is ca. 550 cc). Although $O_2(^1\Sigma_g^+)$, $O_2(^1\Delta_g)$, and other excited O_2 species may be formed in the electrical discharge of O_2 [6,26], they are deactivated by O_2 long before reaching the fluorescence cell, because of the high O_2 concentra-

tion. For example, the lifetime of $O_2(^1\Delta_g)$ is only ca. 1.5 ms at P_{O2} = 500 torr, and O atom has a lifetime of only ca. 7 μs at this pressure. These lifetimes are much shorter than the time (ca. 1 s) it takes for the mixture to flow into the cell. A static system is used for the second method of operation. Gases are admitted to the cell in the order of their desired pressures, with minor component first. In order to ensure complete mixing, the gases are injected into the cell from the two ends simultaneously and about 10 min are allowed for mixing, prior to the beginning of an experiment.

For the studies with O_2 and O_3, both flowing and static systems were employed, and the results show no significant differences. For the other experiments, only the static system was used. In the static measurements, the ozone loss during the many repetitive laser shots limits the length of the experimental runs. For accurate kinetic measurements, ozone losses must be negligible. Therefore many species cannot be studied by this technique, because the reaction(s) of $O(^1D)$ with these species can produce radicals that react catalytically with ozone. Nevertheless, H_2O was investigated, because water vapor is so efficient in deactivating $O_2(^1\Sigma_g^+)$ that only a small amount of H_2O is needed to obtain accurate measurement of the deactivation rate constant, and therefore the small ozone loss can be tolerated. CF_4 was also studied because previous studies have indicated that only physical quenching of $O(^1D)$ occurs [27]. In the measurements presented here, ozone loss was always less than 4% during experiments and will not affect the results significantly.

Results and Discussion

Previous studies have shown that $O(^1D) + O_2$ produces excited $O_2(^1\Sigma_g^+,v)$ in its v = 0 and 1 states at comparable rates [4,11,12,20]. The v = 1 state emits at 771 nm for its (1-1) transition [11]. The monochromator was scanned between 710 nm and 850 nm with several spectral resolutions, and the only emission band observed is the (0-0) band at 762 nm. The absence of the 771 nm feature is because $O_2(^1\Sigma_g^+,v = 1)$ has a very short lifetime in this system: previous studies indicate that the v = 1 state of $O_2(^1\Sigma_g^+)$ is deactivated by O_2 with a rate constant of about 2×10^{-11} cm^3 s^{-1} [4,11,12,20]. A low resolution spectrum of the 762 nm band is shown in Figure 2, and the band halfwidth is in agreement with the calibrated monochromator transmission.

A typical 762 nm fluorescence decay signal is shown in Figure 3, following subtraction of the scattered laser light signal. The scattered light signal is obtained in a separate run in which no O_3 is present in the cell. The solid line is a nonlinear least square fit [28] of the data to an exponential function, using the data points following the ca. 0.6 μsec risetime. In order to test for possible deviations from single exponential decay behavior, a double exponential function was fitted to the data, the parameters obtained confirm that a single exponential function fits the data very well, with no significant second component.

The decay constant, k_I, obtained from least square fit is the pseudo-first order rate constant for the deactivation of $O_2(^1\Sigma_g^+)$, and the initial intensity

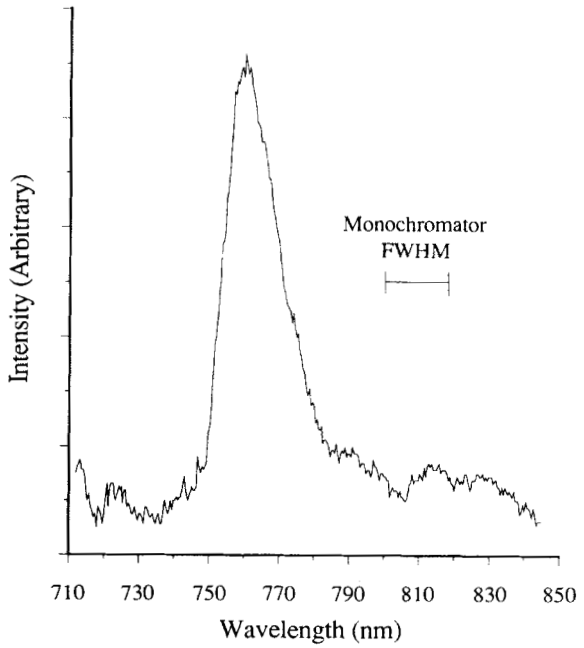

Figure 2. Low resolution spectrum of the 762 nm band of $O_2(^1\Sigma_g^+)$. (monochromator transmission full width at half maximum (FWHM) = 18 nm).

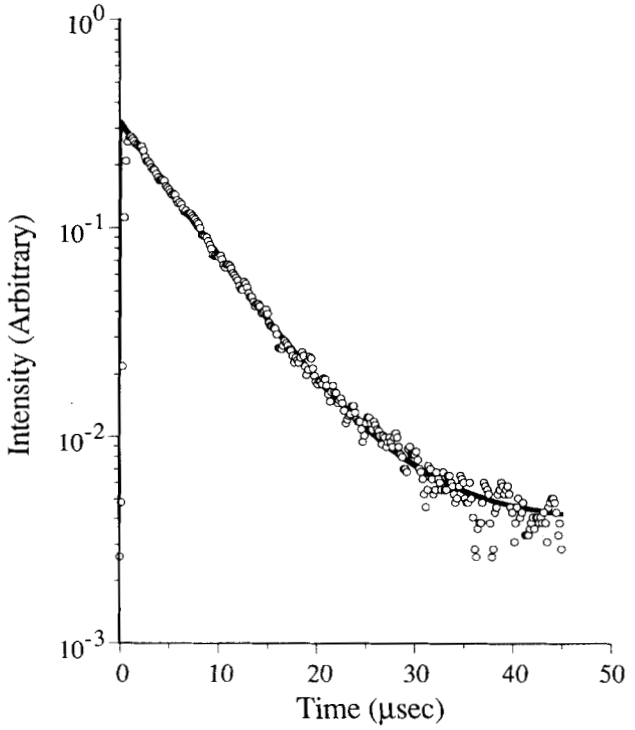

Figure 3. Typical 762 nm fluorescence signal (300 torr of O_2 and 0.45 torr of O_3). The solid line is the least square fit of the signal to an exponential function with background.

is proportional to the concentration of $O_2(^1\Sigma_g^+)$ in the system prior to collisional deactivation. The formation and deactivation of $O_2(^1\Sigma_g^+)$ can be described by the following reactions:

(2) $$O_3 + h\nu\ (308\ nm) \longrightarrow O(^1D) + O_2(^1\Delta_g)$$

$$O(^1D) + M \longrightarrow O(^3P) + M$$

(3) $$O(^1D) + O_2 \longrightarrow O(^3P) + O_2(^1\Sigma_g^+)$$

(4) $$O_2(^1\Sigma_g^+) + M \longrightarrow O_2(^3\Sigma_g^- \text{ or } {}^1\Delta_g) + M$$

(5) $$O_2(^1\Sigma_g^+) + O_3 \longrightarrow 2O_2 + O$$

(6) $$O_2(^1\Sigma_g^+) + O_2 \longrightarrow O_2(^1\Delta_g) + O_2$$

(7) $$O_2(^1\Delta_g) + O_2(^1\Delta_g) \longrightarrow O_2(^1\Sigma_g^+) + O_2(^3\Sigma_g^-)$$

where M represents any quenchers other than O_3 and O_2. Since O_2 is always in great excess compared to O_3 and it is about 1/3 as efficient as O_3 in deactivating $O(^1D)$ [29], quenching by O_3 can be neglected. Wall deactivation of $O_2(^1\Sigma_g^+)$ is very slow on the time scale of this study and has also been neglected. $O_2(^1\Sigma_g^+)$ can also be produced by the energy pooling reaction of $O_2(^1\Delta_g)$, which is produced in the photolysis of O_3 and in the quenching of $O_2(^1\Sigma_g^+)$ by molecules such as O_2 and N_2 [30]. Borrell, Borrell, Grant, and Pedley [31] studied the energy pooling reaction at several temperatures, and determined the rate constant to be 2.0×10^{-17} cm^3 s^{-1} at 295 K. This reaction is too slow to be important in the present experiment, where the $O_2(^1\Delta_g)$ concentration never exceeds 10^{13} cm^{-3}.

Simple steady-state analysis gives the decay constant and the initial fluorescence intensity as:

(8) $$k_1 = k_5[O_3] + k_6[O_2] + k_4[M]$$

(9) $$I = \alpha N_{O^*} \frac{k_3 P_{O2}}{k_3 P_{O2} + k_2 P_M}$$

Here, O* denotes $O(^1D)$ and N_{O^*} is the number density of $O(^1D)$ produced in the photolysis. α is a proportionality constant. In all the measurements carried out in this study, only <0.1% of the ozone is excited in each laser shot, and therefore N_{O^*} is directly proportional to the product of O_3 pressure times the laser intensity (in front of the observing window), as was confirmed experimentally. The normalized intensity I_0 is obtained by dividing the observed intensity I by P_{O3} and laser fluence W_0, giving:

(10) $$I_0 = \frac{I}{P_{O3} W_0} = \frac{k_3 P_{O2}}{A(k_3 P_{O2} + k_2 P_M)}$$

and:

(11) $$\frac{1}{I_0} = A\left(1 + \frac{k_2}{k_3 P_{O2}} P_M\right)$$

Here A is a constant which is proportional to the normalized 762 nm intensity at $P_M = 0$ torr. The relative efficiency of deactivation of $O(^1D)$ by M with respect to that of O_2, $k = k_2/k_3$, can be obtained from eq. (11).

Deactivation of $O_2(^1\Sigma_g^+)$

For the measurements involving only O_3 and O_2, the deactivation rate of $O_2(^1\Sigma_g^+)$ by O_3 is obtained by measuring k_I as a function of $[O_3]$ at fixed O_2 concentration. The k_I vs. $[O_3]$ data at P_{O2} = 300 torr are presented in Figure 4. An excellent linear relation is obtained, where the slope gives the deactivation rate constant of $O_2(^1\Sigma_g^+)$ by O_3. Furthermore, the decay rate by O_2 alone is obtained by subtracting that due to O_3 from the total k_I. The results are presented in Figure 5, where it is obvious that O_2 is very inefficient in quenching $O_2(^1\Sigma_g^+)$, and only an upper limit of 10^{-16} cm^3 s^{-1} can be obtained for the O_2 deactivation rate constant.

For the measurements in which a third species, M, is present, the first order deactivation rate constant of $O_2(^1\Sigma_g^+)$ by M can be calculated by:

$$k_M = k_I - k_5[O_3] - k_6[O_2] \tag{12}$$

Plots of k_M vs. the concentration of M have been obtained in this study for N_2, CO_2, H_2O, CF_4, and all the rare gases, and they are presented in Figures 5 to 9. For inefficient colliders such as the rare gases, k_M is obtained from the difference between two large numbers, and this introduces uncertainty in k_M and the resulting second order rate constants. But, as shown in the figures, good linear relationships are obtained for k_M vs. [M] for all the quenchers. The error bars are obtained from propagation of errors in the other terms of eq. (8). In the case of H_2O, as shown in Figure 6, there is a statistically significant nonzero intercept in the k_M vs. [M] relation. This may be due to the difficulties associated with measuring water vapor pressure. An additional water vapor pressure of only ca. 0.16 torr can account

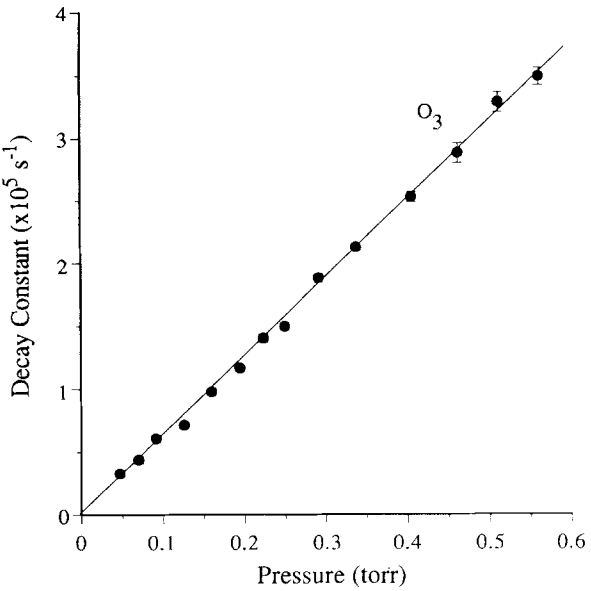

Figure 4. The 762 nm decay constant as a function of O_3 concentration at P_{O2} = 300 torr.

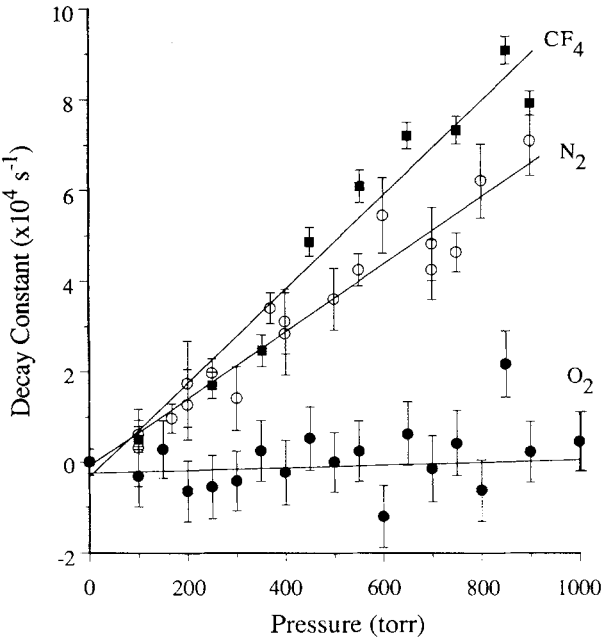

Figure 5. Decay constants as functions of collider concentrations.

for the intercept, and it may be due to water condensed on the cell walls prior to the addition of gases into the cell.

Second order rate constants for deactivation of $O_2(^1\Sigma_g^+)$ are summarized in Table I, along with some representative rate constants reported by other

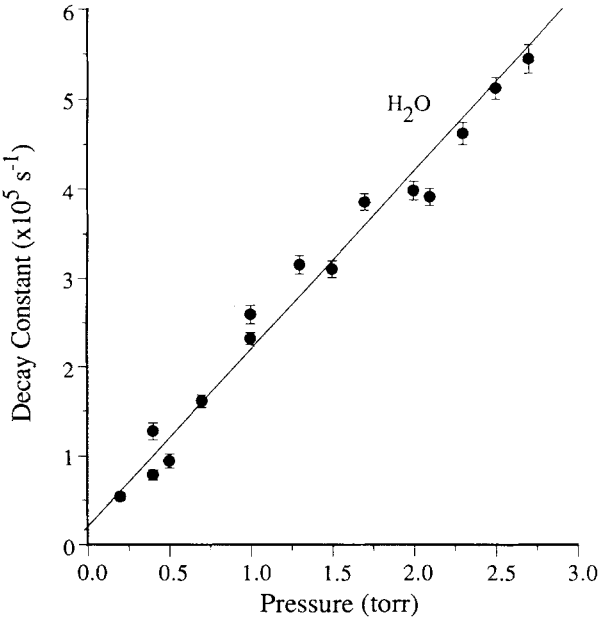

Figure 6. Decay constant as a function of H_2O concentration.

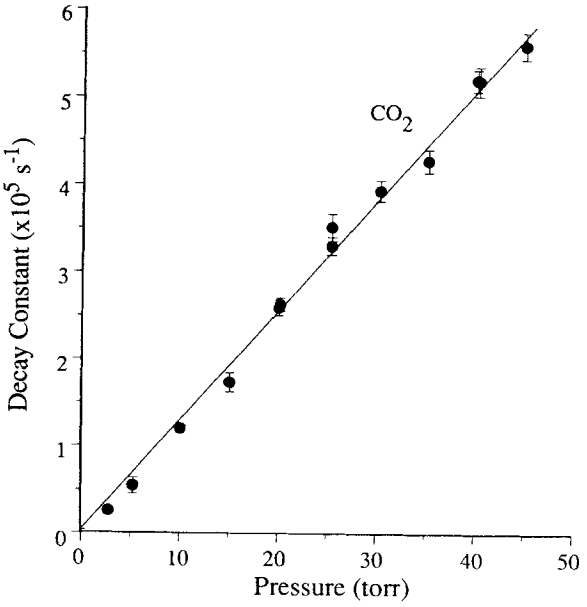

Figure 7. Decay constant as a function of CO_2 concentration.

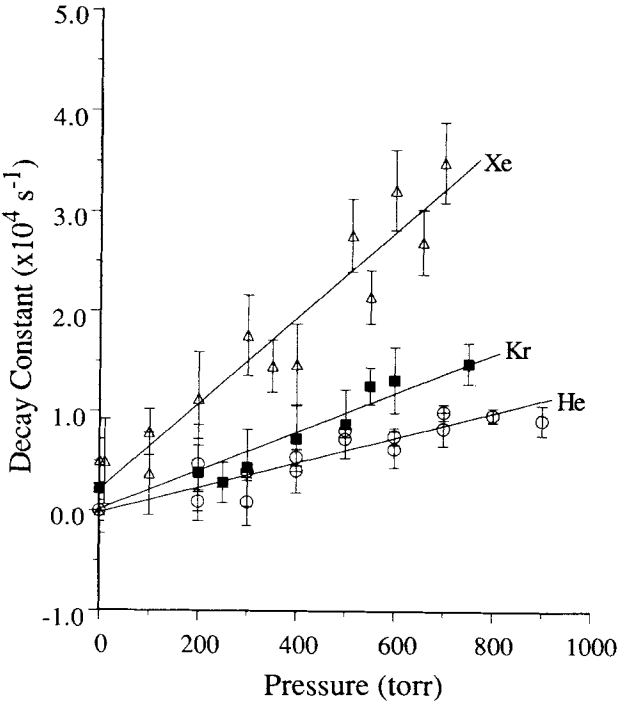

Figure 8. Decay constants as functions of collider concentrations.

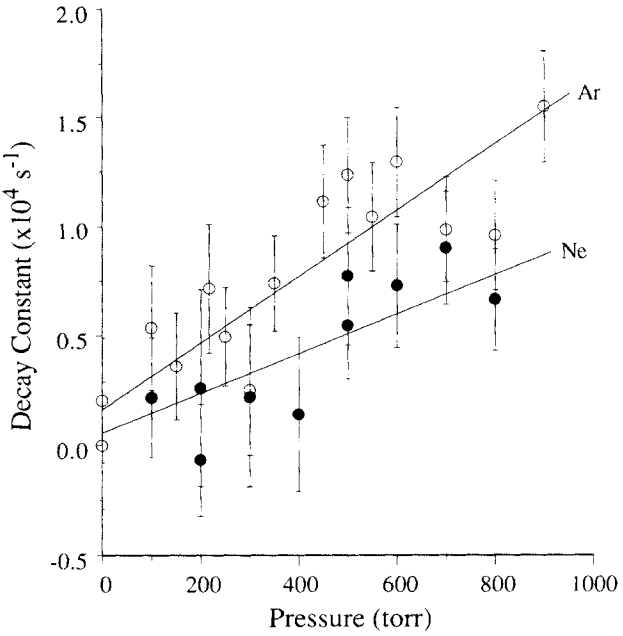

Figure 9. Decay constants as functions of collider concentrations.

workers. For a more complete summary of previous $O_2(^1\Sigma_g^+)$ kinetic studies, readers are referred to a recent review by Wayne [6]. The uncertainties quoted for the present study are $\pm 1\sigma$, based on statistical errors; systematic errors are not considered.

The results from the present study agree reasonably well with previous investigations, except for the rare gases. For CO_2, the present rate constant agrees well with the recent IUPAC recommended value [29], but is larger than those reported by Wildt, Bednarek, Fink, and Wayne [13] and by Singh and Setser [14] in recent studies. The cause for the disagreement is unknown, but it is not likely due to the presence of trace water vapor, because ca. 3% of water impurity would be required in order to make our result consistent with that of Wildt, et al. [13], but the water content is less than 20 ppm in the CO_2 gas used in this study, according to the manufacturer's specifications (Matheson).

There exist in the literature very few determinations of the $O_2(^1\Sigma_g^+)$ deactivation rate constants by rare gases (see Table I), and our rate constants are significantly larger than most of the studies. Filseth, Zia, and Welge [32] measured the rate constants for all the rare gases, but complications were present in their study. The time scale for their measurements was on the order of milliseconds, and the energy pooling reaction of $O_2(^1\Delta_g)$ may have affected the measurements. Moreover, the formation of ozone in their system also seriously complicated the kinetics of $O_2(^1\Sigma_g^+)$. Filseth, et al. [32] reported significant nonlinearity in the O_2 quenching: the O_2 rate constants obtained at high O_2 pressures agree with the presently accepted value, but those obtained at low O_2 pressure are about an order of magnitude larger. Their measurements for the rare gases were carried out at low O_2 pressures,

TABLE I. Summary of $O_2(^1\Sigma_g^+)$ quenching rate constants.

Quencher	Rate Constant ($cm^3.s^{-1}$)	Reference
O_3	$(7.1 \pm 0.8) \times 10^{-12}$	Izod and Wayne [9]
	$(2.5 \pm 0.5) \times 10^{-11}$	Gilpin, et al. [38]
	$(2.2 \pm 0.2) \times 10^{-11}$	Slanger and Black [19]
	$(1.8 \pm 0.2) \times 10^{-11}$	Amimoto and Wiesenfeld[20]
	$(1.8 \pm 0.3) \times 10^{-11}$	Ogren, et al. [39]
	$(2.2 \pm 0.3) \times 10^{-11}$	Choo and Leu[10]
	$(1.96 \pm 0.03) \times 10^{-11}$	this work*
O_2	$(4.6 \pm 1.3) \times 10^{-17}$	Thomas and Thrush [40]
	$(4.0 \pm 0.4) \times 10^{-17}$	Martin, et al.[41]
	$(2.5 \pm 0.2) \times 10^{-17}$	Chatha, et al.[33]
	5.6×10^{-17}	Knickelbein, et al.[30]
	$< 1.0 \times 10^{-16}$	this work*
N_2	2.2×10^{-15}	Stuhl and Welge [42]
	$(2.0 \pm 0.5) \times 10^{-15}$	Noxon [43]
	$(2.2 \pm 0.1) \times 10^{-15}$	Martin, et al.[41]
	$(1.7 \pm 0.08) \times 10^{-15}$	Chatha, et al. [33]
	$(1.7 \pm 0.1) \times 10^{-15}$	Choo and Leu[10]
	$(2.32 \pm 0.14) \times 10^{-15}$	this work*
CO_2	$(4.2 \pm 0.4) \times 10^{-13}$	Davidson, et al. [44]
	$(2.3 \pm 1.2) \times 10^{-13}$	Gauthier and Snelling [45]
	$(4.53 \pm 0.29) \times 10^{-13}$	Aviles, et al. [46]
	$(5.0 \pm 0.3) \times 10^{-13}$	Muller and Houston [18]
	$(4.6 \pm 0.5) \times 10^{-13}$	Choo and Leu[10]
	$(3.0 \pm 1.0) \times 10^{-13}$	Singh and Setser[14]
	$(2.4 \pm 0.4) \times 10^{-13}$	Wildt, et al.[13]
	$(4.0 \pm 0.1) \times 10^{-13}$	this work*

*Statistical uncertainties: $\pm 1\sigma$.

TABLE I. (continued)

H_2O	3.3×10^{-12}	Filseth, et al.[32]
	$(4.0 \pm 0.6) \times 10^{-12}$	O'Brein and Myers [47]
	$(5.0 \pm 1.0) \times 10^{-12}$	Becker, et al.[8]
	$(5.1 \pm 2.1) \times 10^{-12}$	Gauthier and Snelling [45]
	$(6.71 \pm 0.53) \times 10^{-12}$	Aviles, et al.[46]
	$(6.0 \pm 0.3) \times 10^{-12}$	this work*
CF_4	$(2.7 \pm 0.3) \times 10^{-15}$	Davidson, et al.[44]
	$(3.24 \pm 0.26) \times 10^{-15}$	this work*
He	$\sim 1.0 \times 10^{-16}$	Filseth, et al.[32]
	$< 1.0 \times 10^{-16}$	O'Brien and Myers [47]
	$\sim 1.0 \times 10^{-17}$	Becker, et al.[8]
	$(2.0 \pm 0.2) \times 10^{-16}$	Chatha, et al.[33]
	$(2.5 \pm 0.9) \times 10^{-16}$	this work*
Ne	$\sim 1.0 \times 10^{-16}$	Filseth, et al.[32]
	$(3.6 \pm 0.9) \times 10^{-16}$	this work*
Ar	5.8×10^{-18}	Filseth, et al.[32]
	$< 1.0 \times 10^{-16}$	O'Brien and Myers [47]
	$< 2.8 \times 10^{-15}$	Gilpin, et al.[38]
	1.5×10^{-17}	Becker, et al.[8]
	$(4.7 \pm 0.7) \times 10^{-16}$	this work*
Kr	$\sim 1.0 \times 10^{-16}$	Filseth, et al.[32]
	$(5.8 \pm 0.9) \times 10^{-16}$	this work*
Xe	$\sim 1.0 \times 10^{-16}$	Filseth, et al [32]
	$(1.26 \pm 0.17) \times 10^{-15}$	this work*

and the added rare gas pressure may have promoted further O_3 formation through the recombination reaction. Due to these potential complications, the lack of agreement of the present results with those of Filseth, et al. [32] is not surprising.

Becker, Groth, and Schurath [8] also studied the quenching of $O_2(^1\Sigma_g^+)$ by He and Ar in a complex steady state system, but as pointed out in their article, they experienced problems associated with wall losses. They normalized their results to Noxon's rate constant (1.5×10^{-16} cm^3 s^{-1}) [43] for the quenching of $O_2(^1\Sigma_g^+)$ by O_2, but this value is about 3 times larger than that presently accepted. Nonetheless, as discussed by Wayne [6], the quenching rate constants from Becker, et al. agree well with other studies for colliders such as N_2, CO_2, and H_2O. Wayne commented [6] that the agreement may be fortuitous, due to similar levels of H_2O impurities in the various studies.

Efforts were made in the present study to avoid the possible complications from trace H_2O, especially for the rare gases which are several orders of magnitude less efficient in deactivating $O_2(^1\Sigma_g^+)$. All the rare gases are slowly flowed through a silica gel trap at -78°C before being admitted to the cell. At dry ice temperature (-78°C), the saturated water vapor pressure is ca. 4 mtorr, and the maximum quenching rate constant due to the water impurity is only ca. 800 s^{-1}, which is smaller than the scatter in the experimental quenching rate constants for rare gases between 200–1000 torr (see Figs. 8 and 9), and cannot cause significant errors in the results. As shown in Table I, our result for $O_2(^1\Sigma_g^+)$ + He agrees very well with that of Chatha, Arora, Raja, Kulkarni, and Vohra [33].

The present results indicate that the $O_2(^1\Sigma_g^+)$ quenching efficiencies by rare gases increase monotonically from He to Xe. This correlation may provide more insight into the details of the deactivation of $O_2(^1\Sigma_g^+)$. As indicated in the introduction, a curve crossing mechanism explains the temperature dependence of these processes correctly. According to the Landau-Zener formulation [34], the efficiency of the electronic quenching process depends on the intermolecular distances at the curve crossing point, R_x. For the rare gases, R_x may increase from He to Xe. Other factors such as the slope of the potential energy surface at R_x may vary in the same way. Although more studies are needed, the observed trend in the $O_2(^1\Sigma_g^+)$ quenching efficiencies by rare gases may be consistent with the curve crossing description for the $O_2(^1\Sigma_g^+)$ quenching process.

Deactivation of $O(^1D)$

The relative deactivation efficiency of $O(^1D)$ by the collider gases with respect to O_2 can be obtained by eq. (11), if the added collider can change the normalized initial fluorescence intensity I_0 significantly, and the ratio k_2/k_3 can be calculated from the slope and intercept in the $1/I_0$ vs. P_M relation. Rate constant k_3, the deactivation rate constant of $O(^1D)$ by O_2, has been determined in several previous studies. For the present work, we have adopted the result from Amimoto, Force, Gulotty, and Wiesenfeld [35]: $(4.2 \pm 0.2) \times 10^{-11}$ cm^3 s^{-1}, which is recommended in the most recent IUPAC evaluation [29].

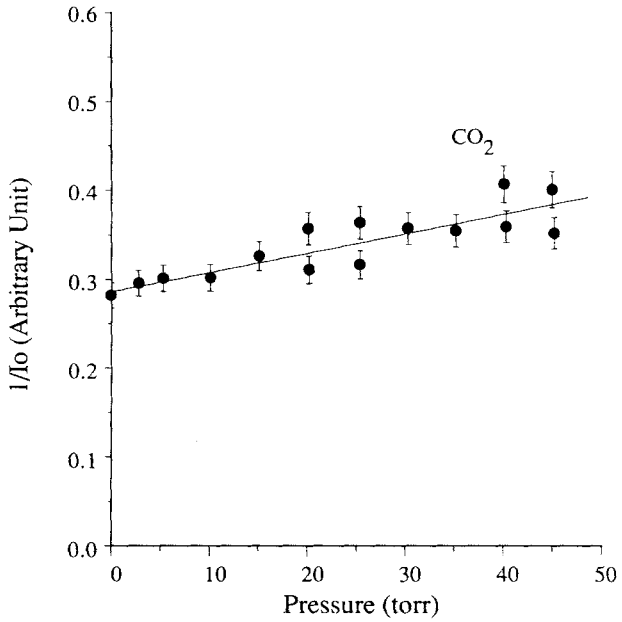

Figure 10. Plot of 1/Io vs. P_M (eq. (11) in text) for CO_2 at P_{O2} = 300 torr.

Plots of $1/I_0$ vs. P_M for CO_2, N_2, Xe, and Kr are shown in Figures 10 and 11, and excellent linear relationships are evident. For colliders such as Ar, Ne, He, and CF_4, which are inefficient in competing with O_2 for $O(^1D)$, $1/I_0$ is essentially constant within experimental error and only upper limits for quenching rate constants can be estimated. The results summarized in

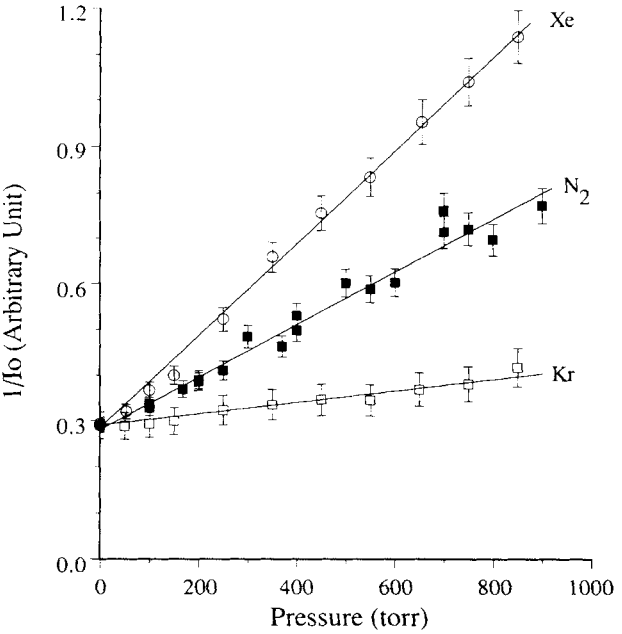

Figure 11. Plot of 1/Io vs. P_M (eq. (11) in text) at P_{O2} = 300 torr.

Table II show excellent agreement with previous studies for N_2, CO_2, Xe, and Kr. For the less efficient colliders, the estimated upper limits to the rate constants are consistent with previous studies, except for that of CF_4, which differs with results given by Fletcher and Husain [36], but is in agreement with that from Force and Wiesenfeld [27] and Schofield [37].

TABLE II. Summary of $O(^1D)$ quenching rate constants.

Quencher	Rate Constant ($cm^3.s^{-1}$)	Reference
O_2	$(7.0 \pm 0.5) \times 10^{-11}$	Heidner, et al.[48]
	$(3.7 \pm 0.7) \times 10^{-11}$	Davidson, et al. [49]
	4.5×10^{-11}	Streit, et al.[50]
	$(4.2 \pm 0.2) \times 10^{-11}$	Amimoto, et al.[35]
N_2	$(2.8 \pm 0.6) \times 10^{-11}$	Davidson, et al.[49]
	$(2.4 \pm 0.1) \times 10^{-11}$	Amimoto, et al.[35]
	$(2.52 \pm 0.25) \times 10^{-11}$	Wine and Ravishankara [51]
	$(2.6 \pm 0.3) \times 10^{-11}$	this work*
CO_2	1.2×10^{-10}	Streit, et al.[50]
	$(1.0 \pm 0.2) \times 10^{-10}$	Schofield [37]
	$(1.28 \pm 0.07) \times 10^{-10}$	Amimoto, et al.[35]
	$(1.04 \pm 0.1) \times 10^{-10}$	Wine and Ravishankara [51]
	$(1.05 \pm 0.18) \times 10^{-10}$	this work*
He	$< 7.0 \times 10^{-16}$	Heidner and Husain [52]
	$< 3.0 \times 10^{-15}$	Schofield [37]
	$< 3.0 \times 10^{-13}$	this work*
Ne	$(1.1 \pm 0.1) \times 10^{-14}$	Heidner and Husain [52]
	$(5.0 \pm 2.0) \times 10^{-15}$	Schofield [37]
	$< 3.0 \times 10^{-13}$	this work*
Ar	$(7.1 \pm 0.06) \times 10^{-13}$	Heidner and Husain [52]
	$(3.0 \pm 2.0) \times 10^{-13}$	Schofield [37]
	$< 5.0 \times 10^{-13}$	this work*

*Statistical uncertainties: $\pm 1\sigma$.

TABLE II. (continued)

Kr	$(1.55\pm0.13) \times 10^{-11}$	Heidner and Husain [52]
	$(6.6 \pm 1.0) \times 10^{-12}$	Schofield [37]
	$(4.9 \pm 0.7) \times 10^{-12}$	this work*
Xe	$(1.0 \pm 0.1) \times 10^{-10}$	Heidner and Husain [52]
	$(7.2 \pm 1.4) \times 10^{-11}$	Schofield [37]
	$(5.0 \pm 0.5) \times 10^{-11}$	this work*
CF_4	$(1.2 \pm 0.1) \times 10^{-11}$	Fletcher and Husain[36]
	(1.7 ± 0.3) x 10-13	Schofield[37]
	$(1.8 \pm 0.1) \times 10^{-13}$	Force and Wiesenfeld[27]
	$< 6.0 \times 10^{-13}$	this work*

Conclusions

The laser flash photolysis technique has been used to study the kinetics of the deactivation of $O_2(^1\Sigma_g^+)$ by O_3, O_2, N_2, CO_2, H_2O, CF_4, and the rare gases in real time measurements. Rate constants have been obtained for all quenchers except O_2, for which only an upper limit is obtained. The resulting rate constants agree with previous studies except for the rare gases, for which very few measurements are available from previous studies. The observed variation in the $O_2(^1\Sigma_g^+)$ quenching efficiencies from He to Xe are consistent with the proposition that this electronic quenching process proceeds via a curve crossing mechanism. Measurements are also reported for deactivation rate constants of $O(^1D)$ by N_2, CO_2, Xe, and Kr; for other colliders used in this study, only upper limits can be estimated. These rate constants are in good agreement with literature values.

Acknowledgment

The authors thank T.G. Slanger and I.C. McDade for helpful discussions, and W.R. Skinner for providing several optical filters. This research was supported in part by the Department of Energy (Office of Basic Energy Sciences).

Bibliography

[1] R.P. Wayne, *J. Photochem.*, **25,** 345 (1984).
[2] A. Bucholtz, W.R. Skinner, V.J. Abreu, and P.B. Hays, *Planet. Space Sci.*, **34,** 1031 (1986).
[3] K. Henriksen, G.G. Sivjee, C.S. Deehr, and H.K. Myrabo, *Planet. Space Sci.*, **33,** 119 (1985).
[4] T.G. Slanger, *Can. J. Phys.*, **64,** 1657 (1986); and reference therein.

[5] E. A. Ogryzlo, Y.Q. Shen, and P.T. Wassell, *J. Photochem.*, **25,** 389 (1984).
[6] R. P. Wayne, *Singlet O_2*, A. A. Frimer, Ed., CRC press, Boca Raton, 1985, Vol. 1, p. 81.
[7] P. M. Borrell, P. Borrell, and K. R. Grant, *J. Chem. Phys.*, **78,** 748 (1983).
[8] K. H. Becker, W. Groth, and U. Schurath, *Chem. Phys. Lett.*, **8,** 259 (1971).
[9] T. P. Izod and R. P. Wayne, *Proc. Roy. Soc.*, **A308,** 81 (1968).
[10] K.Y. Choo and M-T. Leu, *Int. J. Chem. Kinet.*, **17,** 1155 (1985).
[11] L.C. Lee and T.G. Slanger, *J. Chem. Phys.*, **69,** 4053 (1978).
[12] M. J. E. Gauthier and D. R. Snelling, *Can. J. Chem.*, **57,** 4007 (1974).
[13] J. Wildt, G. Bednarek, E. H. Fink, and R. P. Wayne, *Chem. Phys.*, **122,** 463 (1988).
[14] J. P. Singh and D.W. Setser, *J. Phys. Chem.*, **89,** 5353 (1985).
[15] K. Kear and E.W. Abrahamson, *J. Photochem.*, **3,** 409 (1975).
[16] M. Braithwaite, J. A. Davidson, and E. A. Ogryzlo, *J. Chem. Phys.*, **65,** 771 (1976); and *Ber. Bunsenges. Phys. Chem.*, **81,** 179 (1977).
[17] E. A. Ogryzlo and B. A. Thrush, *Chem. Phys. Lett.*, **24,** 314 (1974).
[18] D. F. Muller and P. L. Houston, *J. Phys. Chem.*, **85,** 3563 (1981).
[19] T.G. Slanger and G. Black, *J. Chem. Phys.*, **70,** 3434 (1979).
[20] S. T. Amimoto and J. R. Wiesenfeld, *J. Chem. Phys.*, **72,** 3899 (1980).
[21] W.T. Rawlins, G. E. Caledonia, and R. A. Armstrong, *J. Chem. Phys.*, **87,** 5209 (1987).
[22] J. Shi and J. R. Barker, *J. Phys. Chem.* (in press).
[23] E. H. Fink, H. Kruse, D. A. Ramsay, and M. Vervloet, *Can. J. Phys.*, **64,** 242 (1986).
[24] L.T. Molina and M. J. Molina, *J. Geophys. Res.*, **91,** 14501 (1986).
[25] J. Barnes and K. Mauersberger, *J. Geophys. Res.*, **92,** 14864 (1987).
[26] H. Sugimitsu and S. Okazaki, *J. Chim. Phys.*, **79,** 655 (1982).
[27] A. P. Force and J. R. Wiesenfeld, *J. Phys. Chem.*, **85,** 782 (1981).
[28] P. R. Bevington, *Data Reduction and Error Analysis for Physical Science,* McGraw Hill, New York, 1969, p. 237.
[29] R. Atkinson, D. L. Baulch, R. A. Cox, R. F. Hampson, J. A. Kerr, and J. Troe, *J. Phys. Chem. Ref. Data,* **18,** 881 (1989).
[30] M. B. Knickelbein, K. L. Marsh, O. E. Ulrich, and G. E. Busch, *J. Chem. Phys.*, **87,** 2392 (1987).
[31] M. B. Borrell, P. Borrell, K. R. Grant, and D. Pedley, *J. Phys. Chem.*, **86,** 700 (1982).
[32] S.V. Filseth, A. Zia, and K. H. Welge, *J. Chem. Phys.*, **52,** 5502 (1970).
[33] J. P. G. Chatha, P. K. Arora, S. N. Raja, P. J. B. Kulkarni, and K.G. Vohra, *Int. J. Chem. Kinet.*, **11,** 175 (1979).
[34] J.T. Yardley, *Introduction to Molecular Energy Transfer,* Academic, New York, 1980, p. 212.
[35] S.T. Amimoto, A. P. Force, R.G. Gulotty, and J. R. Wiesenfeld, *J. Chem. Phys.*, **71,** 3640 (1979).
[36] I. S. Fletcher and D. Husain, *J. Phys. Chem.*, **80,** 1837 (1976).
[37] K. Schofield, *J. Photochem.*, **9,** 55 (1978); and references therein.
[38] R. Gilpin, H. I. Schiff, and K. H. Welge, *J. Chem. Phys.*, **55,** 1087 (1971).
[39] P. J. Ogren, T. J. Sworski, C. J. Hochanadel, and J. M. Cassel, *J. Phys. Chem.*, **86,** 238 (1982).
[40] R. G. O. Thomas and B. A. Thrush, *J. Chem. Soc. Faraday Trans. II,* **71,** 664 (1975).
[41] L. R. Martin, R. B. Cohen, and J. Schatz, *Chem. Phys. Lett.*, **41,** 394 (1976).
[42] F. Stuhl and K. H. Welge, *Can. J. Chem.*, **47,** 1870 (1969).
[43] J. F. Noxon, *J. Chem. Phys.*, **52,** 1852 (1970).
[44] J. A. Davidson, K. E. Kear, and E.W. Abrahamson, *J. Photochem.*, **1,** 307 (1973).
[45] M. Gauthier and D. R. Snelling, *J. Photochem.*, **4,** 27 (1975).
[46] R. G. Aviles, D. F. Muller, and P. L. Houston, *Appl. Phys. Lett.*, **37,** 358 (1980).
[47] R. J. O'Brien and G. H. Myers, *J. Chem. Phys.*, **53,** 3832 (1970).
[48] R. F. Heidner, D. Husain, and J. R. Wiesenfeld, *J. Chem. Soc. Faraday Trans. II,* **69,** 927 (1973).
[49] J. A. Davidson, H. I. Schiff, G. E. Streit, J. R. McAfee, A. L. Schmeltekopf, and C. J. Howard, *J. Chem. Phys.*, **67,** 5021 (1977).
[50] G. E. Streit, C. J. Howard, A. L. Schmeltekopf, J. A. Davidson, and H. I. Schiff, *J. Chem. Phys.*, **65,** 4761 (1976).

[51] P. H. Wine and A. R. Ravishankara, *Chem. Phys. Lett.*, **77,** 103 (1981).
[52] R. F. Heidner and D. Husain, *Int. J. Chem. Kinet.*, **6,** 77 (1974).

Received June 4, 1990
Accepted July 20, 1990